Fish and Shellfish Immunology 93 (2019) 766–780

Contents lists available at ScienceDirect

Fish and Shellfish Immunology

journal homepage: www.elsevier.com/locate/fsi

Full length article

Global profiling and characterization of Japanese flounder (*Paralichthys olivaceus*) kidney microRNAs regulated by *Edwardsiella tarda* infection in a time-dependent fashion

Wen-rui Li[a,b,c], Yong-hua Hu[d], Shuai Jiang[a,b], Li Sun[a,b,*]

[a] CAS Key Laboratory of Experimental Marine Biology, CAS Center for Ocean Mega-Science, Institute of Oceanology, Chinese Academy of Sciences, Qingdao, China
[b] Laboratory for Marine Biology and Biotechnology, Pilot National Laboratory for Marine Science and Technology (Qingdao), China
[c] University of Chinese Academy of Sciences, Beijing, China
[d] Institute of Tropical Bioscience and Biotechnology, Chinese Academy of Tropical Agricultural Sciences, Haikou, China

ARTICLE INFO

Keywords:
microRNA
Paralichthys olivaceus
Edwardsiella tarda
Infection

ABSTRACT

Japanese flounder (*Paralichthys olivaceus*) is an important economic fish species farmed in China and other countries. It is susceptible to infection by *Edwardsiella tarda*, a severe fish pathogen with a broad host range. In this study, we employed high-throughput deep sequencing technology to identify, in a global scale, flounder kidney microRNAs (miRNAs) induced by *E. tarda* at different stages of infection. Differentially expressed miRNAs (DEmiRNAs) and mRNAs (DEmRNAs) exhibiting significantly altered expression levels before and after *E. tarda* infection were examined. A total of 96 DEmiRNAs were identified, for which 2779 target genes were predicted. Eighty-seven miRNA–mRNA pairs, involving 29 DEmiRNAs and 86 DEmRNAs, showed negative correlations in their expression patterns. GO and KEGG enrichment analysis revealed that the putative target genes of the DEmiRNAs were associated with diverse biological processes, cellular components, and molecular functions. One of the DEmiRNAs, pol-miR-182-5p, was demonstrated to regulate sphingosine-1-phosphate receptor 1 (PoS1PR1) negatively in a manner that depended on the specific interaction between the seed sequence of pol-miR-182-5p and the 3'-UTR of PoS1PR1. Overexpression of pol-miR-182-5p in flounder cells promoted apoptosis and inhibited cellular viability. Knockdown of PoS1PR1 in flounder enhanced *E. tarda* invasion and dissemination in fish tissues. These results provide new insights into miRNA-mediated anti-bacterial immunity in flounder.

1. Introduction

MicroRNAs (miRNAs) are a type of small non-coding RNAs with approximately 22 nucleotides that regulate mRNA stability and translation in post-transcriptional stages [1,2]. MiRNAs modulate gene expression mostly through binding the 3′- untranslated region (UTR) of target genes, resulting in mRNA degradation or protein translation repression [3–5]. Extensive studies indicate that miRNAs are involved in many cellular and biological processes such as cell development, cell apoptosis, cell viability and immune response [6–9].

MiRNAs have been demonstrated to play a vital role during microbial infection in various animal models. In fish, miRNAs associated with pathogen infection have been identified in a number of species [10–18]. In Japanese flounder (*Paralichthys olivaceus*), reports have shown that the miRNA pol-miR-194a served as a target for bacterial manipulation of host immune defense by suppressing the expression of type I interferon; pol-miR-7a regulated PI3K/AKT/GSK3β 39 signaling pathway by inhibiting the expression of insulin receptor substrate-2 (IRS2a and IRS2b) during bacterial infection; pol-miR-731 facilitated megalocytivirus infection by negatively regulating type I interferon response, apoptosis, and cell cycle arrest [10–12]. In grouper (*Epinephelus coioides*) and miiuy croaker (*Miichthys miiuy*), a number of miRNAs were found to be involved in bacterial and viral infection through regulating inflammatory responses, cell apoptosis, and NF-κB activation [13–18].

Edwardsiella tarda is a Gram-negative bacteria and a pathogen with a wide host range that includes mammals, birds, reptiles, and fish [19–23]. In aquaculture, *E. tarda* causes heavy economic losses and is widely accepted as a severe pathogen. *E. tarda* can infect a large number of marine and freshwater fish, including Japanese flounder, turbot, tongue sole, tilapia, and carp [24–27]. Unlike most aquaculture bacterial pathogens, *E. tarda* is capable of intracellular invasion and

* Corresponding author. Institute of Oceanology, Chinese Academy of Sciences, 7 Nanhai Road, Qingdao, 266071, China.
E-mail address: lsun@qdio.ac.cn (L. Sun).

https://doi.org/10.1016/j.fsi.2019.07.078
Received 23 May 2019; Received in revised form 22 July 2019; Accepted 26 July 2019
Available online 14 August 2019

evading host immunity [28,29]. It possesses sophisticated virulence-associated systems, including two-component systems, quorum-sensing system, secretory systems, and regulators such as Fur and Hfq [19–23]; the cross-talks between these systems/regulators enable *E. tarda* to sense changes in the environment, regulate the expression of virulence genes, and succeed in host infection [19–21]. However, the interaction processes between *E. tarda* and fish hosts as well as the underlying mechanisms are largely unclear.

Like many fish species, Japanese flounder is susceptible to *E. tarda* infection. Recent reports showed that *E. tarda* infection affected the expression of a large amount of flounder proteins and induced differential expression of 17 miRNAs in the liver of flounder [12,30]. In the present study, we investigated flounder miRNAs expressed in head kidney during *E. tarda* infection at different time points by high-throughput deep sequencing technology. MiRNAs differentially expressed after *E. tarda* infection as well as their putative target genes were identified based on combined analysis of the miRNAs and mRNAs sequence data. From the obtained miRNA libraries, one miRNA, pol-miR-182-5p, was further examined for its regulation mechanism and effect on *E. tarda* infection.

2. Materials and methods

2.1. Fish maintenance

Clinically healthy Japanese flounder were purchased from a commercial fish farm and maintained in the laboratory for two weeks 22 °C in aerated seawater as reported previously [10]. For small RNA sequencing and bacterial infection, the fish used were 10 months old, with an average weight of 200.4 g; for all other experiments, the fish used were 4 months old, with an average weight of 20.2 g. Before experiment, the fish were verified to be clinically healthy as reported previously [31]. Before tissue collection, fish were euthanized with an overdose of tricaine methanesulfonate (Sigma, St. Louis, MO, USA) as reported previously [32].

2.2. Preparation of head kidney samples for high-throughput sequencing

Edwardsiella tarda TX01 was isolated from diseased fish in a fish farm in China and cultured in Luria-Bertani broth (LB) at 28 °C as reported previously [33] to an OD_{600} of 0.8, the cells were washed with PBS (pH 7.4) and resuspended in PBS to 5×10^7 CFU/ml. Japanese flounder (average weight 200.4 g) were divided randomly into two groups and injected intraperitoneally (i.p.) with 200 μL bacterial suspension or PBS. Head kidney was taken from the fish (three at each time point) at 0, 12, 24 and 48 h post-bacterial infection (hpi); bacterial recovery from the tissue sample at each time point was determined by plate count as reported previously [34]. Equal amounts of tissue samples from three fish at each time-point were pooled together and immediately stored in liquid nitrogen. Head kidney samples of each time point (0, 12, 24, and 48 hpi) were then used for subsequent small RNA sequencing.

2.3. Sequencing of small RNAs

Small RNA isolation, library construction, and high throughput sequencing were all performed by Novogene Company (Beijing, China). Clean reads were obtained by removing reads containing poly-N, with 5′ adapter contaminants, without 3' adapter or the insert tag, containing poly A or T or G or C and low quality reads from raw reads. The small RNA tags were mapped to reference sequence by Bowtie program without mismatch. miRBase20.0 was used to look for known miRNA through mapped small RNA tags. The characteristics of hairpin structure of miRNA precursors were used to predict novel miRNA. miREvo and mirdeep2 were integrated to predict novel miRNA through exploring the secondary structure, the Dicer cleavage site and the minimum free energy of the small RNA tags unannotated in the former steps. MiRNA expression levels were estimated by TPM (transcript per million) through the following criteria: Normalized expression = mapped readcount/Total reads*1000000. Analysis of differential expression of miRNA was performed using DESeq R package. The P-values were adjusted using Benjamini & Hochberg method. Corrected P-value of 0.05 was set as the threshold for significantly differential expression by default. Prediction of miRNA target gene was performed by miRanda, PITA and RNAhybrid. Enrichment analysis of the predicted target genes was conducted with Gene Ontology (GO) (http://www.geneontology.org/) and KEGG pathway (http://www.genome.jp/kegg/). The raw sequencing data have been deposited at the National Center for Biotechnology Information (BioProject accession number PRJNA541203).

2.4. Stem–loop RT-PCR and quantitative real-time PCR (qRT-PCR)

To examine miRNAs expression in flounder kidney during *E. tarda* infection, head kidney samples of different infection time were prepared as described above. MiRNAs were extracted from the samples using miRNAiso plus kit (TaKaRa, Dalian, China) and used for cDNA synthesis with specific stem-loop reverse transcription (RT) primer (5′-GTCGTATCCAGTGCAGGGTCCGAGGTATTCGCACTGGATACGAC-3′) and miRNA first-strand cDNA synthesis kit (Vazyme, Nanjing, China) according to the manufacturer's protocol. MiRNAs expression was determined by qRT-PCR using comparative threshold cycle method ($2^{-\Delta\Delta CT}$) as reported previously [34,35]. The primers used in the PCR are listed in Table S1. The abundance of miRNAs was normalized relative to that of 5S rRNA as reported previously [35,36]. The experiment was performed independently three times. To examine the effect of megalocytivirus on the expression of pol-miR-182-5p, flounder were injected intraperitoneally (i.p.) with megalocytivirus RBIV-C1 (10^5 copies/fish) as described previously [34,35]. Fish (three at each time point) were euthanized at 2, 4, 6, 8, and 10 days post-infection (dpi), and head kidney was collected and used for examination of pol-miR-182-5p expression as above.

2.5. miRNA mimic

pol–miR-182-5p mimic and pol-miR-182-5p mimic-M, which is pol-miR-182-5p mimic with the seed sequence (5′-UUGGCAA-3′) mutated to its complementary sequence (5′-AACCGUU-3′), were synthesized by GenePharma (Shanghai, China). The negative control, pol-miRNA-NC, was designed and synthesized by the same company.

2.6. Cell culture

FG-9307, a cell line established from Japanese flounder gill cells, were cultured at 24 °C in L-15 (Thermo Scientific HyClone, USA) containing 10% fetal bovine serum (FBS) (Gibco, Invitrogen Corp., USA) and 100 units/ml penicillin and 100 pg/ml streptomycin (Beyotime Biotechnology, China) [36,37]. HEK293T human embryonic kidney epithelial cells (CBTCCCAS, Shanghai, China) were cultured in DMEM (Invitrogen, Grand Island, USA) supplemented with 10% FBS and 100 units/ml penicillin and 100 pg/ml streptomycin in a humidified atmosphere of 37 °C and 5% CO_2.

2.7. Apoptosis and cellular viability assays

Transfection of FG-9307 cells with miRNA mimic was performed as reported previously [37,38]. Briefly, FG-9307 cells were cultured as above in 6-well plates. To examine the effect of pol-miR-182-5p on cellular apoptosis, FG-9307 cells (4×10^5 cells/well) were transfected with or without (control) 200 nM pol-miR-182-5p mimic or pol-miR-NC using Lipofectamine™ 3000 (Invitrogen, Carlsbad, USA) for 48 h. The transfected cells were digested with trypsin, collected, and then washed

twice with PBS. The cells were resuspended in binding buffer and treated with fluorescein isothiocyanate (FITC)-conjugated annexin V for 10 min and then treated with propidium iodide (PI) for 5 min in the dark according to the manufacturer's instructions (Solarbio, Beijing, China). The cells were subjected to flow cytometry using a FACS Flow Cytometer (BD Biosciences, USA). Data analysis was performed using FlowJo software 7.6.1 (Tree Star Inc, Ashland, USA).

To measure cellular viability, FG-9307 cells were cultured in 96-well plates (10^4 cells/well) and transfected with or without (control) 200 nM pol-miR-182-5p mimic or pol-miR-NC using Lipofectamine™ 3000 as above. At 24, 48, 72, and 96 h after transfection, cellular viability was recorded by incubating with CCK-8 (KeyGen BiotechCo, Nanjing, China) at 24 °C for 2 h, followed by measuring absorbance at 450 nm.

2.8. Determination of PoS1PR1 as a target gene of pol-miR-182-5p

For luciferase reporter assay, the plasmids pMIR-182-5p-3′UTR$_{PoS1PR1}$ and pMIR-182-5p-3′UTR$_{PoS1PR1}$-Mut were constructed. pMIR-182-5p-3′UTR$_{PoS1PR1}$, which contains the firefly luciferase gene with its 3′-UTR replaced by the 3′-UTR of PoS1PR1, was constructed as follows: the 3′-UTR of PoS1PR1 was amplified by PCR with the primers F1 (5′- TGATGAAAGCTGCGCACTAGTGGACATAGACTAGTCCAT-3′) and R1 (5′-AAAAGATCCTTTATTAAGCTTTGAATAGAAAGCTAA AGT-3′); the PCR products were inserted into the luciferase vector pMIR-Reporter (AmBio, Life Technologies, USA) at the Spe I/Hind III sites, resulting in pMIR-182-5p-3′UTR$_{PoS1PR1}$. pMIR-182-5p-3′UTR$_{PoS1PR1}$-Mut is identical to pMIR-182-5p-3′UTR$_{PoS1PR1}$, except that the sequence of the 3′-UTR of PoS1PR1 complementary to pol-miR-182-5p seed sequence was mutated to its complementary sequence by overlap PCR with the primers F2 (5′-AACGGTTAAAATGAAACTG CAG-3′) and R2 (5′-TTCATTTTAACCGTTAACCATTTATTGTGC-3′).

To determine the interaction between pol-miR-182-5p and 3′-UTR of PoS1PR1 (3′UTR$_{PoS1PR1}$), HEK293T cells were transfected with pMIR-182-5p-3′UTR$_{PoS1PR1}$ alone, or with pMIR-182-5p-3′UTR$_{PoS1PR1}$ plus pol-miR-182-5p mimic, pMIR-182-5p-3′UTR$_{PoS1PR1}$ plus pol-miR-NC using Lipofectamine™ 3000 (Invitrogen, Carlsbad, USA) according to the manufacturer's instructions. At 24 h post transfection, the cells were lysed, and luciferase activity was measured using a firefly luciferase reporter gene assay kit (Beyotime Biotechnology, China) according to the manufacturer's instructions with β-galactosidase as an internal control.

To examine the specificity of the interaction between pol-miR-182-5p and 3′-UTR$_{PoS1PR1}$, HEK293T cells were transfected with pMIR-182-5p-3′UTR$_{PoS1PR1}$ alone, pMIR-182-5p-3′UTR$_{PoS1PR1}$ plus pol-miR-182-5p mimic, pMIR-182-5p-3′UTR$_{PoS1PR1}$ plus pol-miR-NC, pMIR-182-5p-3′UTR$_{PoS1PR1}$ plus pol-miR-182-5p mimic-M, or pMIR-182-5p-3′UTR$_{PoS1PR1}$-M plus pol-miR-182-5p mimic. Luciferase activity was determined as above. All experiments were performed three times.

To examine the effect of pol-miR-182-5p on the expression of PoS1PR1, FG-9307 cells were transfected with or without pol-miR-182-5p mimic or pol-miR-NC as above, and PoS1PR1 expression was determined by qRT-PCR as above.

2.9. Sequence analysis

The amino acid sequence of PoS1PR1 (GenBank accession no. XP_019963867.1) was analyzed using the BLAST program at the National Center for Biotechnology Information (NCBI). The theoretical molecular mass and isoelectric point were predicted with ProtParam tool. Domain search was performed with the simple modular architecture research tool (SMART) and the conserved domain search program of NCBI. Pairwise sequence alignment was created with European Molecular Biology Open Software Suite (EMBOSS). Multiple sequence alignment was created with DNAMAN.

2.10. PoS1PR1 knockdown and its effect on E. tarda infection

PoS1PR1 knockdown was performed by small RNA (siRNA) interference as reported previously [38, 39]. To select effective siRNAs for PoS1PR1, three siRNAs targeting PoS1PR1 were inserted into the siRNA expression vector pRNAT-CMV3.1 (GenScript, Piscataway, USA) between BamH I/Alf II sites, resulting in plasmids pPoS1PR1si-1, pPoS1PR1si-2, and pPoS1PR1si-3. The plasmid pPoS1PR1siC, which expresses a scramble siRNA, was constructed similarly. To examine the interfering efficiency of the siRNAs, four groups of flounder were injected intramuscularly with pPoS1PR1siC, pPoS1PR1si-1, pPoS1PR1si-2, or pPoS1PR1si-3, at the dose of 15 μg/fish; the control group of fish was injected with PBS. At 3, 5 and 7 d post-plasmid injection, head kidney, spleen and liver were taken aseptically. The tissues were used for total RNA extraction with RNAiso plus kit (TaKaRa, Dalian, China), and cDNA synthesis was performed with First Strand cDNA Synthesis Kit (TOYOBO, Japan) according to the manufacturer's protocol. The expression of PoS1PR1 in head kidney, spleen and liver were determined by qRT-PCR as described above with beta-actin as an internal reference [39,40]. The plasmid showing the strongest inhibitory effect on PoS1PR1 expression was re-named pPoS1PR1si. The siRNA sequences expressed by pPoS1PR1si and pPoS1PR1siC are 5′- GACAGTC ACCATTGTGCTG-3′ and 5′-ATTGTCAGCGCGCTAAGCT-3′, respectively.

To examine the effect of PoS1PR1 knockdown on *E. tarda* infection, flounders (average weight 20.2 g) were divided randomly into three groups and injected with pPoS1PR1si, pPoS1PR1siC, or PBS (control). At 5 d post-plasmid administration, fish were infected with 100 μL *E. tarda* (10^7 CFU/ml). At 12, 24, and 48 hpi, head kidney, spleen and liver were taken from the fish (three at each time point) and examined for bacterial recovery by plate count as reported previously [40,34].

2.11. Statistical analysis

All experiments were performed at least three times, and statistics analysis was carried out with GraphPad Prism 5 (GraphPad Software, USA). The statistical analysis and the p-values are indicated in the figures.

3. Results

3.1. Identification of flounder head kidney miRNAs induced by E. tarda infection at different time points

To examine flounder head kidney miRNA expression at different time points of *E. tarda* infection, four small-fragment RNA libraries corresponding to 0, 12, 24, and 48 hpi were constructed and subjected to high-throughput sequence analysis. Bacterial recovery analysis showed that the numbers of *E. tarda* in head kidney increased steadily from 12 hpi to 48 hpi (Fig. S1). A total of 12,064,305, 11,691,505, 11,869,600 and 10,359,148 small fragment reads were obtained in the 0, 12, 24, and 48 hpi libraries, respectively, of which, 15.71%, 15.51%, 14.12% and 19.17% reads were mapped to known miRNAs in miRBase 20.0, and 33.59% (0 hpi), 34.45% (12 hpi), 36.63% (24 hpi) and 27.45% (48 hpi) of the reads mapped to the hairpin structures of the flounder genome were identified as novel miRNAs (Fig. 1A). There were 817 miRNAs identified, which included 781 novel miRNAs (Table S2). Among these miRNAs, 40.98%, 43.25%, 38.32% and 39.82% from the 0, 12, 24, and 48 hpi libraries, respectively, were 22-nt in sequence (Fig. 1B).

3.2. Differentially expressed miRNAs (DEmiRNA) during E. tarda infection

The expression profiles of the 817 miRNAs were normalized by TPM. The results showed that 296 miRNAs were expressed at all examined time points, and, of these miRNAs, 29, 33, 31, and 23 were

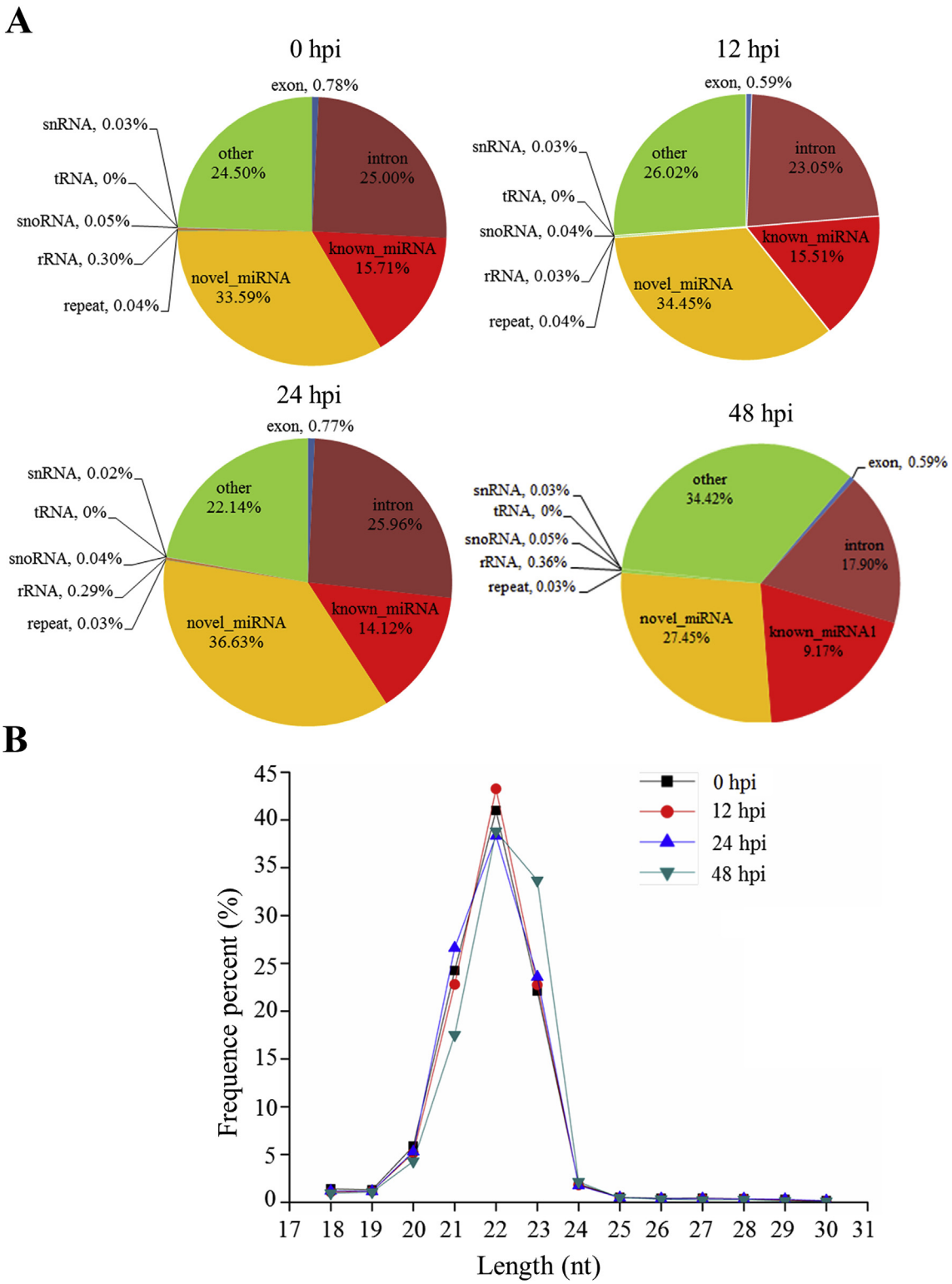

Fig. 1. Japanese flounder small RNAs identified at different time points after *Edwardsiella tarda* infection. (A) Composition of the small RNAs. (B) Length distribution of the small RNAs. nt: nucleotide.

specifically expressed at 0, 12, 24, and 48 hpi, respectively. (Fig. 2A). Compared to their expression levels at 0 hpi, 96 miRNAs showed significant ($P < 0.05$) differences in expression after bacterial infection (Tables 1–3) and were named DEmiRNAs. At 12 hpi, 10 and 17 miRNAs were significantly upregulated and downregulated, respectively; at 24 hpi, 10 and 14 miRNAs were significantly upregulated and downregulated, respectively; at 48 hpi, 27 and 35 miRNAs were significantly upregulated and downregulated, respectively (Fig. 2B). Two miRNAs showed differential expressions at all time points, while 18, 16, and 47 miRNAs altered expressions only at 12, 24, and 48 hpi, respectively (Fig. 2C). Specifically, pol-miR-novel_182 and pol-miR-novel_131 displayed steadily downregulated and upregulated expressions, respectively, after bacterial infection. The expressions of five novel miRNAs, i.e., pol-miR-novel_258, pol-miR-novel_200, pol-miR-novel_1206, pol-

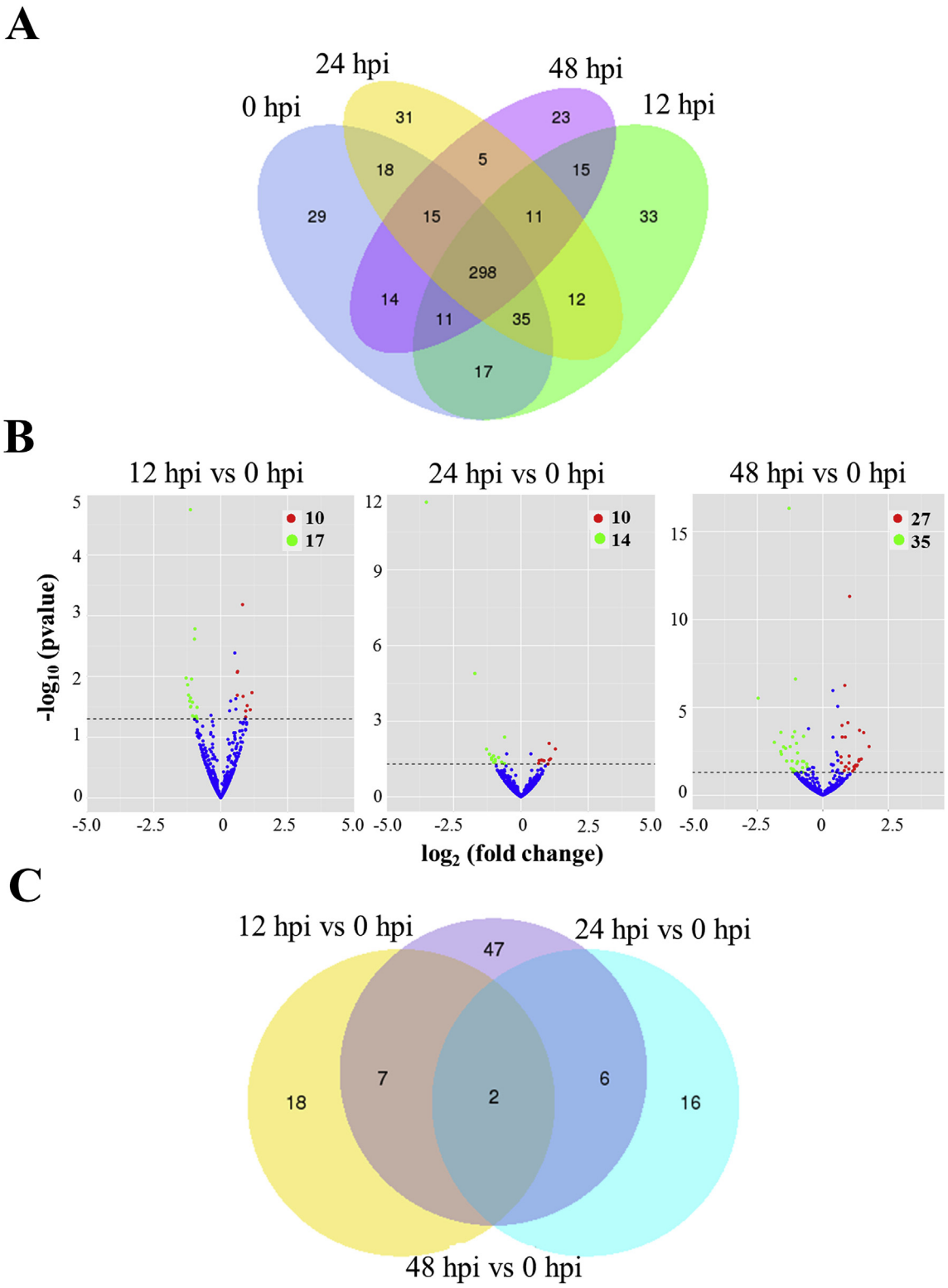

Fig. 2. Flounder miRNA expression during *Edwardsiella tarda* infection. (A) Venn diagram showing miRNA expression at 0, 12, 24, and 48 hpi. The numbers inside the diagram stand for the numbers of miRNAs. (B) Volcanic plots of differential expression of miRNAs at 12, 24, and 48 hpi in comparison to that at 0 hpi. Red and green spots represent miRNAs significantly ($P < 0.05$) upregulated and downregulated, respectively. (C) Venn diagram showing differentially expressed miRNAs (DEmiRNAs) expression at different time. The numbers inside the diagram stand for the numbers of DEmiRNAs. (For interpretation of the references to colour in this figure legend, the reader is referred to the Web version of this article.)

miR-novel_1284 and pol-miR-novel_1288, were first downregulated at 12 hpi, became comparable to control level at 24 hpi, and then were downregulated again at 48 hpi; the expressions of pol-miR-novel_79 and pol-miR-182-5p were upregulated at 12 and 48 hpi. The expressions of the novel miRNAs of pol-miR-novel_957, pol-miR-novel_423, and pol-miR-novel_685 were downregulated at 24 and 48 hpi, while the expressions of pol-miR-novel_796, pol-miR-novel_159, and pol-let-7b-3p were upregulated at 24 and 48 hpi (Tables 1–3). The

Table 1
Differential expression of flounder miRNAs at 12 h post infection (hpi).

miRNA	12 hpi readcount	0 hpi readcount	log2 Fold change	P value
pol-miR-novel_182	98.74196	228.8698	−1.1313	1.79E-05
pol-miR-novel_201	85.17351	47.13384	0.81642	0.000654
pol-miR-novel_1000	791.0897	1651.685	−0.96237	0.001644
pol-miR-novel_258	14.27644	30.86364	−0.97955	0.002422
pol-miR-novel_47	24227.69	15229.51	0.63287	0.008233
pol-miR-novel_5	646836.5	410727.4	0.62027	0.008534
pol-miR-novel_867	0	2.972512	−1.2929	0.010573
pol-miR-novel_863	9.064572	23.97174	−1.0877	0.011032
pol-miR-novel_1130	3.155705	12.59574	−1.2362	0.01375
pol-miR-novel_547	2.380386	0	1.1682	0.018462
pol-miR-novel_269	6.055314	26.38461	−1.202	0.020261
pol-miR-novel_79	726.0496	457.4393	0.61971	0.020356
pol-miR-novel_244	21.47438	11.10136	0.83658	0.021283
pol-miR-novel_833	0	2.241925	−1.1272	0.022575
pol-miR-novel_342	0.911979	8.008192	−1.1585	0.025486
pol-miR-novel_352	4.042233	11.52517	−1.0558	0.026595
pol-miR-182-5p	1043.67	416.5752	0.98871	0.030189
pol-miR-novel_200	27.62795	106.3426	−1.1163	0.031071
pol-miR-novel_1206	0.734203	3.856963	−1.1274	0.031691
pol-miR-novel_1284	6.495063	14.28584	−0.88544	0.032298
pol-miR-novel_1103	3.591137	0.626888	1.104	0.035294
pol-miR-novel_131	1584.707	676.3218	0.93378	0.036992
pol-miR-novel_315	2.034622	10.68212	−1.0522	0.044394
pol-miR-novel_181	0	5.214564	−0.91529	0.04512
pol-miR-novel_447	1.976283	0	0.93261	0.046425
pol-miR-novel_1288	4.759213	13.16897	−0.97	0.046825
pol-miR-novel_838	5.116324	11.93215	−0.88613	0.049319

Table 2
Differential expression of flounder miRNAs at 24 h post infection (hpi).

miRNA	24 hpi readcount	0 hpi readcount	log2 Fold change	P value
pol-miR-novel_947	0	53.84381	−3.5094	2.07E-12
pol-miR-novel_172	66.79273	283.7328	−1.7099	1.28E-05
pol-miR-novel_957	734.7654	1139.514	−0.60513	0.004254
pol-miR-novel_854	24.35568	9.924631	1.0472	0.00755
pol-miR-novel_796	5.258116	0.673452	1.2799	0.012591
pol-miR-novel_1097	0.945425	7.388118	−1.2775	0.012794
pol-miR-novel_423	0.280263	3.925921	−1.1688	0.020243
pol-miR-novel_255	4.381077	11.61065	−1.016	0.023703
pol-miR-novel_183	56.33701	111.3108	−0.82896	0.027337
pol-miR-novel_171	21.89368	74.54741	−1.0899	0.028498
pol-miR-novel_467	4.69629	0.686278	1.0994	0.030871
pol-miR-novel_298	1.613188	6.727491	−1.0889	0.032661
pol-miR-novel_1008	0	12.52753	−0.95355	0.03318
pol-miR-novel_861	8.301066	2.588945	1.0479	0.03451
pol-miR-novel_264	37.0285	20.11909	0.76169	0.034616
pol-let-7b-3p	509.0501	299.429	0.67989	0.035916
pol-miR-novel_131	1345.391	663.8775	0.83229	0.035994
pol-miR-novel_159	352.6042	167.5186	0.858	0.036729
pol-miR-novel_685	0	2.265045	−0.95767	0.039007
pol-miR-novel_182	126.4636	223.4876	−0.71453	0.041514
pol-miR-novel_448	0.3849	3.222791	−1.0135	0.042731
pol-miR-novel_1073	29.74536	17.7952	0.65766	0.046538
pol-miR-novel_19	36013.51	57567.08	−0.60917	0.047742
pol-miR-novel_124	2274.87	616.1507	1.0057	0.04935

expression patterns of 12 DEmiRNAs were validated by stem-loop RT-PCR analysis (Fig. S2), which showed that the expression profiles of these 12 miRNAs were essentially similar to those determined by high-throughput deep sequencing.

3.3. Differentially expressed mRNAs (DEmRNA) during E. tarda infection

Parallel to miRNAs analysis, global changes in mRNAs expression in the course of*E. tarda* infection were also examined through RNA-Seq analysis. The results showed that 1872, 1773, and 3018 mRNAs exhibited significantly ($P < 0.05$) different expressions at 12, 24, and 48 hpi, respectively (Fig. S3). These mRNAs were named DEmRNAs. Specifically, 1092 and 782 mRNAs were significantly upregulated and downregulated, respectively, at 12 hpi; 1024 and 749 mRNAs were significantly upregulated and downregulated, respectively, at 24 hpi; 1777 and 1241 mRNAs were significantly upregulated and down-regulated, respectively, at 48 hpi (Fig. S3).

Table 3
Differential expression of flounder miRNAs at 48 h post infection (hpi).

miRNA	48 hpi readcount	0 hpi readcount	log2 Fold change	P value
pol-miR-novel_875	18877.16	46959.12	−1.2898	4.68E-17
pol-miR-221-3p	19564.09	9527.82	1.0198	4.80E-12
pol-miR-124-5p	194.2454	411.2422	−1.044	2.43E-07
pol-miR-199a-3p	78879.01	43550.47	0.83757	5.61E-07
pol-miR-novel_943	1.532928	23.7338	−2.4693	2.98E-06
pol-let-7b-3p	539.3175	269.376	0.95421	7.42E-05
pol-miR-199a-5p	85724.68	50929.59	0.7296	0.000105
pol-miR-novel_137	974.3506	320.6266	1.3975	0.0002
pol-miR-novel_182	90.34189	202.2426	−1.0766	0.000241
pol-miR-novel_223	12.74248	50.50205	−1.6022	0.000264
pol-miR-novel_299	15.92758	4.234781	1.5573	0.000274
pol-miR-novel_2	296384.3	503121.1	−0.73599	0.000444
pol-miR-144-5p	53039.77	128659.3	−1.1562	0.000476
pol-let-7d-3p	119.8126	70.24112	0.736	0.000485
pol-miR-221-5p	2012.915	1077.812	0.85601	0.000489
pol-miR-novel_918	0	5.81641	−1.8518	0.00098
pol-miR-novel_151	314.7466	673.5415	−1.0075	0.001101
pol-miR-21-3p	4.805532	0.316326	1.7637	0.001696
pol-miR-122-5p	158.1335	435.9769	−1.2479	0.001701
pol-miR-novel_1095	6.250693	24.69854	−1.4985	0.001769
pol-miR-novel_157	95.16433	333.8945	−1.4192	0.002147
pol-miR-novel_329	1.092457	7.656975	−1.6073	0.003274
pol-miR-novel_258	13.00291	27.36756	−0.96548	0.003869
pol-miR-novel_1206	0	3.414315	−1.5828	0.004617
pol-miR-182-5p	807.515	367.4367	1.0015	0.005857
pol-miR-novel_79	673.6526	405.149	0.69356	0.00658
pol-miR-novel_1087	17.90601	2.717407	1.4658	0.00863
pol-miR-novel_292	18.41968	4.254886	1.3816	0.009332
pol-miR-novel_127	1589.791	355.6605	1.381	0.010357
pol-miR-novel_1288	4.082952	11.61958	−1.1767	0.011227
pol-miR-novel_395	1.065748	5.756093	−1.3841	0.011343
pol-miR-novel_906	2.876018	0	1.3695	0.011368
pol-miR-novel_167	182.4473	328.4073	−0.77729	0.011859
pol-miR-novel_957	597.9881	1030.838	−0.72949	0.012026
pol-miR-144-3p	9283.578	20134.12	−0.96554	0.012173
pol-miR-22-5p	1089.253	643.4468	0.70592	0.014232
pol-miR-novel_180	171.6264	75.68395	0.99836	0.014523
pol-miR-novel_123	879.6908	1991.016	−0.99281	0.015441
pol-miR-9b-5p	633.4746	993.95	−0.61402	0.016399
pol-miR-novel_1155	11.92547	1.348651	1.3126	0.019244
pol-miR-novel_105	2.202089	0	1.2485	0.019336
pol-miR-novel_389	4.898067	0.800361	1.2867	0.021852
pol-miR-182-3p	16.224	4.847327	1.1847	0.023453
pol-miR-novel_131	1210.374	595.7484	0.88072	0.023529
pol-miR-novel_159	299.3875	150.7791	0.85875	0.024112
pol-miR-novel_64	10515.51	16364.78	−0.59991	0.024673
pol-miR-novel_199	68.48152	125.0931	−0.77483	0.026968
pol-miR-novel_423	0.347935	3.557979	−1.2139	0.029938
pol-miR-novel_209	70.92952	29.73773	0.98917	0.0315
pol-miR-novel_796	4.365062	0.592441	1.204	0.031746
pol-miR-novel_642	0	2.025453	−1.1435	0.032896
pol-miR-novel_1114	0	2.169117	−1.1172	0.035364
pol-miR-novel_22	19.90109	10.13848	0.81596	0.039829
pol-miR-novel_200	23.36659	93.96907	−1.1418	0.040009
pol-miR-novel_1038	4.104894	0.632652	1.1376	0.042202
pol-miR-novel_685	0	2.065664	−1.0542	0.044575
pol-miR-novel_1284	6.33846	12.65292	−0.83281	0.045778
pol-miR-novel_188	23.52613	63.70374	−1.0176	0.046489
pol-miR-novel_1010	0.744522	3.839047	−1.1158	0.047276
pol-miR-novel_1225	3.739784	9.963496	−1.0022	0.047808
pol-miR-novel_278	8.932368	16.52722	−0.76804	0.048697
pol-miR-novel_388	1.08769	5.40057	−1.1061	0.049202

Table 4
Predicted target mRNAs for 12 h upregulated miRNAs.

miRNA	mRNA	Gene description	log2 Fold change	P value
pol-miR-novel_1103	109627028	Transcription factor 7-like 2	1.104	0.035294
pol-miR-novel_1103	109627333	tuberin-like	1.104	0.035294
pol-miR-novel_1103	109641952	Acyl-CoA-binding domain-containing protein 5A	1.104	0.035294
pol-miR-novel_47	109633562	Zinc finger protein 845	0.63287	0.0082333
pol-miR-novel_47	109638351	Methylcytosine dioxygenase TET2	0.63287	0.0082333
pol-miR-novel_5	109640918	Splicing factor 3B subunit 1	0.62027	0.0085339
pol-miR-novel_547	109627028	Transcription factor 7-like 2	1.1682	0.018462
pol-miR-novel_547	109634811	Phosphatidylinositol 3,4,5-trisphosphate 3-phosphatase and dual-specificity protein phosphatase	1.1682	0.018462
pol-miR-novel_547	109637795	Ligand-dependent nuclear receptor corepressor-like protein	1.1682	0.018462
pol-miR-novel_547	109643036	RING finger protein 157	1.1682	0.018462

3.4. DEmiRNAs target genes predicted from DEmRNAs

A total of 2779 target genes were predicted for the 96 DEmiRNAs. By examining the expression patterns of DEmiRNAs and DEmRNAs, 4 upregulated miRNAs and 7 downregulated miRNAs were predicted to target 9 downregulated mRNAs and 16 upregulated mRNAs, respectively, at 12 hpi; at 24 hpi, 3 upregulated miRNAs were predicted to target 16 downregulated genes, and 2 downregulated miRNAs were predicted to target 2 upregulated genes; at 48 hpi, 4 upregulated miRNAs and 10 downregulated miRNAs were predicted to target 19 downregulated mRNAs and 24 upregulated mRNAs, respectively (Tables 4–9). At 12 hpi, the upregulated pol-miR-novel_1103 was predicted to target three genes, i.e., transcription factor 7, acyl-coA-binding doman-containing protein 5A, and tuberin-like (Table 4); the downregulated pol-miR-novel_833 was predicted to target 6 genes, i.e., sigma non-opioid intracellular receptor 1, vezatin, redox-regulatory protein FAM213A, transcription initiation factor IIA subunit 2, Eighteen S rRNA Factor 1 (ESF1), and transmembrane emp24 domain-containing protein 9 (Table 5). At 24 hpi, the upregulated pol-miR-novel_854 was predicted to target 3 genes, i.e., palmitoyltransferase ZDHHC14, cyclin-dependent kinase inhibitor 1B, and telomerase-binding protein EST1A (Table 6), and the downregulated pol-miR-novel_1097 was predicted to target only one gene (mortality factor 4-like protein) (Table 7). At 48 hpi, the upregulated pol-miR-182-5p was predicted to target one gene (sphingosine 1-phosphate receptor 1) (Table 8), while the downregulated pol-miR-124-5p was predicted to target 7 genes (Table 9). In total, 29 DEmiRNAs were predicted to target 86 DEmRNAs, and 87 of the miRNA–mRNA pairs had negative correlations in their expression patterns.

3.5. Enrichment analysis of DEmiRNA target genes

Gene ontology (GO) analysis was performed to examine the DEmiRNA target genes identified above, and the top ten enriched GO terms of Biological Processes, Cellular Component, and Molecular Function are shown in Fig. 3A. In biological processes, 12 hpi DEmiRNAs targets included T cell and B cell receptor signaling pathways, response to acid chemical, maintenance of location, and meiotic DNA double-strand break formation; 24 hpi DEmiRNAs targets included single organism cell adhesion and virion attachment to host cell; 48 hpi DEmiRNAs targets include viral transcription, cytoplasmic microtubule organization, spindle organization, nonmotile primary cilium assembly, and single organism cell adhesion (Fig. 3A). In the category of molecular function, 12 hpi DEmiRNAs targets included RNA-DNA hybrid ribonuclease activity, glucosyltransferase activity, oxidoreductase activity, and protein-disulfide reductase activity; 24 hpi DEmiRNAs targets included acid-amino acid ligase activity, transmembrane receptor protein tyrosine kinase activity, and sodium proton antiporter activity; 48 hpi DEmiRNAs targets included DNA ligase activity. In the category of cellular component, 12 and 24 hpi DEmiRNAs targets included thylakoid membrane and chromosomal region, respectively; 48 hpi DEmiRNAs targets included ciliary base, centrosome, and DNA-directed RNA polymerase II (Fig. 3A).

KEGG pathway analysis showed that the putative target genes of DEmiRNAs were grouped into 60 pathways. The top ten most abundant pathways are shown in Fig. 3B. The 12 hpi DEmiRNAs targets included Wnt signaling pathway, focal adhesion, lysosome, tight junction, p53 signaling pathway, Notch signaling pathway, mTOR signaling pathway, starch/sucrose metabolism, and ECM-receptor interaction. The 24 hpi DEmiRNAs targets included calcium signaling pathway, purine metabolism, melanogenesis, ubiquitin mediated proteolysis, oxidative phosphorylation, ErbB and GnRH signaling pathways, ribosome biogenesis, SNARE interactions in vesicular transport, and fructose/mannose metabolism. The 48 hpi DEmiRNAs targets overlapped in some pathways with 12 and 24 hpi DEmiRNAs targets, such as Notch signaling pathway, purine metabolism, and ubiquitin mediated

Table 5
Predicted target mRNA for 12 h downregulated miRNAs.

miRNA	mRNA	Gene description	log2 Fold change	P value
pol-miR-novel_1288	109632338	Uncharacterized protein	−0.97	0.046825
pol-miR-novel_181	109627043	Mediator of RNA polymerase II transcription subunit 24	−0.91529	0.04512
pol-miR-novel_181	109632026	Uncharacterized protein	−0.91529	0.04512
pol-miR-novel_181	109634113	Nucleobindin-1	−0.91529	0.04512
pol-miR-novel_181	109644194	ER membrane protein complex subunit 3	−0.91529	0.04512
pol-miR-novel_181	109644900	Renalase	−0.91529	0.04512
pol-miR-novel_315	109630328	Tripartite motif-containing protein 3	−1.0522	0.044394
pol-miR-novel_342	109627674	Bifunctional UDP-N-acetylglucosamine 2-epimerase/N-acetylmannosamine kinase	−1.1585	0.025486
pol-miR-novel_833	109626365	Sigma non-opioid intracellular receptor 1	−1.1272	0.022575
pol-miR-novel_833	109640766	Vezatin	−1.1272	0.022575
pol-miR-novel_833	109642672	Redox-regulatory protein FAM213A	−1.1272	0.022575
pol-miR-novel_833	109646123	Transcription initiation factor IIA subunit 2	−1.1272	0.022575
pol-miR-novel_833	109647950	ESF1	−1.1272	0.022575
pol-miR-novel_833	109648056	Transmembrane emp24 domain-containing protein 9	−1.1272	0.022575
pol-miR-novel_838	109630332	Elongation factor G, mitochondrial	−1.1272	0.022575
pol-miR-novel_863	109645724	Serologically defined colon cancer antigen 3	−1.1272	0.022575

Table 6
Predicted target mRNAs for 24 h upregulated miRNAs.

miRNA	mRNA	Gene description	log2 Fold change	P value
pol-miR-novel_796	109623803	Zinc finger C3H1 domain-containing protein	1.2799	0.012591
pol-miR-novel_796	109624666	G/T mismatch-specific thymine DNA glycosylase	1.2799	0.012591
pol-miR-novel_796	109628875	Solute carrier family 2, facilitated glucose transporter member 9	1.2799	0.012591
pol-miR-novel_796	109634192	Histone-lysine N-methyltransferase SUV420H2	1.2799	0.012591
pol-miR-novel_796	109634674	Peroxisome proliferator-activated receptor gamma coactivator 1-alpha	1.2799	0.012591
pol-miR-novel_796	109642520	Extracellular matrix protein FRAS1	1.2799	0.012591
pol-miR-novel_796	109643700	Fibrillin-2	1.2799	0.012591
pol-miR-novel_796	109644845	Nuclear receptor coactivator 1	1.2799	0.012591
pol-miR-novel_854	109628131	Probable palmitoyltransferase ZDHHC14	1.0472	0.0075495
pol-miR-novel_854	109632907	Cyclin-dependent kinase inhibitor 1B	1.0472	0.0075495
pol-miR-novel_854	109635825	Telomerase-binding protein EST1A	1.0472	0.0075495
pol-miR-novel_861	109623793	Vacuolar protein sorting-associated protein 13A	1.0479	0.03451
pol-miR-novel_861	109624689	BANP	1.0479	0.03451
pol-miR-novel_861	109626913	RNA exonuclease 4	1.0479	0.03451
pol-miR-novel_861	109630943	Girdin	1.0479	0.03451
pol-miR-novel_861	109645713	E3 ubiquitin-protein ligase MSL2	1.0479	0.03451

Table 7
Predicted target mRNAs for 24 h downregulated miRNAs.

miRNA	mRNA	Gene description	log2 Fold change	P value
pol-miR-novel_1097	109623915	Mortality factor 4-like protein 1	−1.2775	0.012794
pol-miR-novel_171	109629900	FAM49B	−1.0899	0.028498

Table 8
Predicted target mRNAs for 48 upregulated miRNAs.

miRNA	mRNA	Gene description	log2 Fold change	P value
pol-miR-novel_1087	109625825	Phospholipid hydroperoxide glutathione peroxidase, mitochondrial	1.4658	0.0086298
pol-miR-novel_796	109623957	BET1-like protein	1.204	0.031746
pol-miR-novel_796	109627180	PARG_BOVIN Poly(ADP-ribose) glycohydrolase	1.204	0.031746
pol-miR-novel_796	109628695	Sorting nexin-25	1.204	0.031746
pol-miR-novel_796	109632083	WD and tetratricopeptide repeats protein 1	1.204	0.031746
pol-miR-novel_796	109634192	Histone-lysine N-methyltransferase	1.204	0.031746
pol-miR-novel_796	109635731	Complement component C1q receptor	1.204	0.031746
pol-miR-novel_796	109637717	Claudin domain-containing protein 1	1.204	0.031746
pol-miR-novel_796	109637954	Probable ubiquitin carboxyl-terminal hydrolase FAF-X	1.204	0.031746
pol-miR-novel_796	109638510	Glutathione peroxidase 1	1.204	0.031746
pol-miR-novel_796	109638599	Bromodomain-containing protein 1	1.204	0.031746
pol-miR-novel_796	109639690	Prostaglandin D2 receptor 2	1.204	0.031746
pol-miR-novel_796	109640188	AMP-activated protein kinase subunit gamma-2	1.204	0.031746
pol-miR-novel_796	109642482	Exosome complex component CSL4	1.204	0.031746
pol-miR-novel_796	109646196	Serine/threonine-protein kinase PINK1, mitochondrial	1.204	0.031746
pol-miR-novel_796	109646970	RING finger protein unkempt homolog	1.204	0.031746
pol-miR-novel_796	109647571	Aquaporin FA-CHIP	1.204	0.031746
pol-let-7d-3p	109627584	NK-tumor recognition protein	0.736	0.0004852
pol-miR-182-5p	109627256	Sphingosine 1-phosphate receptor 1	1.0015	0.0058568

proteolysis; the pathways unique to 48 hpi DEmiRNAs targets included glutathione, peroxisome, fatty acid metabolism, and galactose metabolisms.

3.6. Effect of pol-miR-182-5p on cellular apoptosis and viability

As shown in Fig. S2, one of the DEmiRNAs, pol-miR-182-5p, exhibited continued upregulation after *E. tarda* infection at all time points. In addition, our preliminary study with viral infection indicated that in flounder infected with megalocytivirus, pol-miR-182-5p was continuously downregulated (Fig. S4). These results suggested a possibly universal role of pol-miR-182-5p in common pathogen infection. Thus, pol-miR-182-5p was selected for further study. To examine whether pol-miR-182-5p had any effect on the viability status of host cells, flounder FG-9307 cells were transfected with pol-miR-182-5p mimic, and cellular apoptosis and viability were determined at different time points. The results showed that in FG-9307 cells transfected with pol-miR-182-5p mimic, the percentage of apoptotic cells was significantly increased by 2.5 times compared to that of the control cells, whereas in FG-9307 cells transfected with the negative control miRNA, pol-miR-NC, the percentage of apoptotic cells was comparable to that of the control cells (Fig. 4A). Consistently, the amounts of viable cells in FG-9307 transfected with pol-miR-182-5p mimic for 48 h and 72 h were significantly lower than that of the control cells, whereas the numbers of viable cells in FG-9307 transfected with pol-miR-NC were comparable to that of the control cells (Fig. 4B).

3.7. Validation of PoS1PR1 as the target gene of pol-miR-182-5p

P. olivaceus sphingosine-1-phosphate receptor 1 (PoS1PR1) was predicted to be a target gene of pol-miR-182-5p. To examine whether this was indeed the case, the reporter plasmid pMIR-182-5p-3′UTR$_{PoS1PR1}$ was constructed, which contains a firefly luciferase reporter linked to the 3′-UTR of PoS1PR1 (3′UTR$_{PoS1PR1}$) (Fig. S5). When HEK-293T cells were co-transfected with pMIR-182-5p-3′UTR$_{PoS1PR1}$ and pol-miR-182-5p mimic, the luciferase activity was significantly

Table 9
Predicted target mRNAs for 48 h downregulated miRNAs.

miRNA	mRNA	Gene description	log2 Fold change	P value
pol-miR-novel_1114	109635406	Pyruvate dehydrogenase E1 component subunit beta, mitochondrial	−1.1172	0.035364
pol-miR-novel_1114	109635919	CCR4-NOT transcription complex subunit 8	−1.1172	0.035364
pol-miR-novel_151	109643567	Bromodomain testis-specific protein	−1.0075	0.0011008
pol-miR-novel_182	109639367	Galectin-9	−1.0766	0.0002415
pol-miR-novel_188	109643804	Actin-related protein 2-A	−1.0176	0.046489
pol-miR-novel_199	109640565	Splicing factor, proline- and glutamine-rich	−0.77483	0.026968
pol-miR-novel_2	109646156	EH domain-containing protein 4	−0.73599	0.0004445
pol-miR-novel_395	109629756	Poly(U)-binding-splicing factor PUF60	−1.3841	0.011343
pol-miR-novel_395	109631290	SH3 domain-containing RING finger protein 3	−1.3841	0.011343
pol-miR-novel_395	109638179	RNA-binding protein EWS	−1.3841	0.011343
pol-miR-novel_395	109639370	A-kinase anchor protein 1, mitochondrial	−1.3841	0.011343
pol-miR-novel_395	109647317	N-acetylglucosamine-1-phosphodiester alpha-N-acetylglucosaminidase	−1.3841	0.011343
pol-miR-novel_642	109626803	Uncharacterized protein	−1.1435	0.032896
pol-miR-novel_642	109633240	Ubiquitin carboxyl-terminal hydrolase 5	−1.1435	0.032896
pol-miR-novel_642	109644900	Renalase	−1.1435	0.032896
pol-miR-novel_642	109645987	TAF5-like RNA polymerase II p300/CBP-associated factor-associated factor 65 kDa subunit 5L	−1.1435	0.032896
pol-miR-122-5p	109626905	NHL repeat-containing protein 2	−1.2479	0.0017006
pol-miR-124-5p	109623558	Mediator of RNA polymerase II transcription subunit 16	−1.044	2.43E-07
pol-miR-124-5p	109623635	Sorting nexin-2	−1.044	2.43E-07
pol-miR-124-5p	109625764	Synaptotagmin-like protein 4	−1.044	2.43E-07
pol-miR-124-5p	109627698	Phosphatidylinositol 4-kinase type 2-beta	−1.044	2.43E-07
pol-miR-124-5p	109628826	Uncharacterized protein	−1.044	2.43E-07
pol-miR-124-5p	109637623	HAUS augmin-like complex subunit 4	−1.044	2.43E-07
pol-miR-124-5p	109640371	Putative oxidoreductase GLYR1	−1.044	2.43E-07

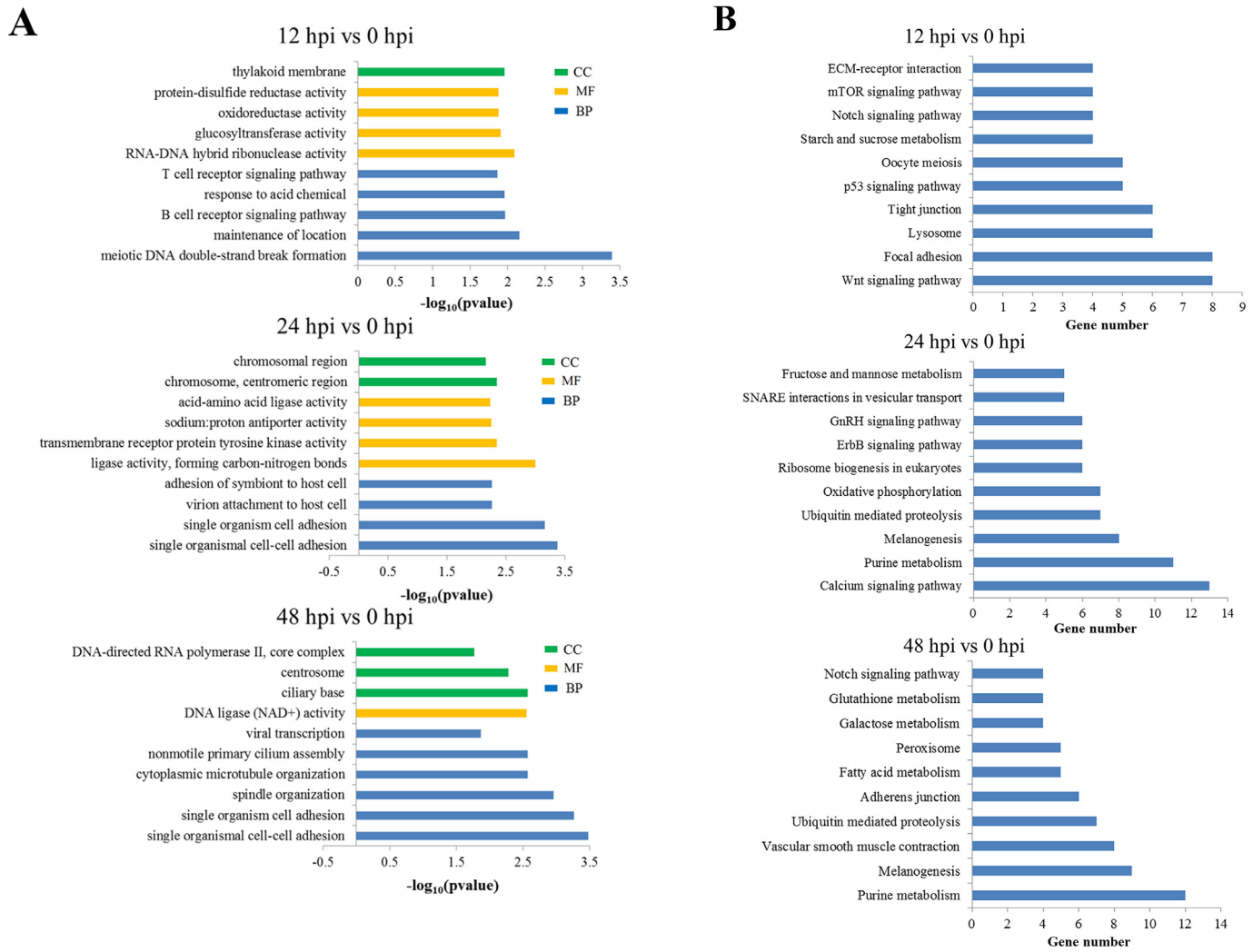

Fig. 3. GO and KEGG analysis of DEmiRNA target genes. (A) Top ten enriched GO terms for the DEmRNAs targeted by DEmiRNAs at 12, 24, and 48 hpi. CC: cellular component, MF: molecular function, BP: biological process. (B) Top ten enriched KEGG pathways for the DEmRNAs targeted by DEmiRNAs at 12, 24, and 48 hpi.

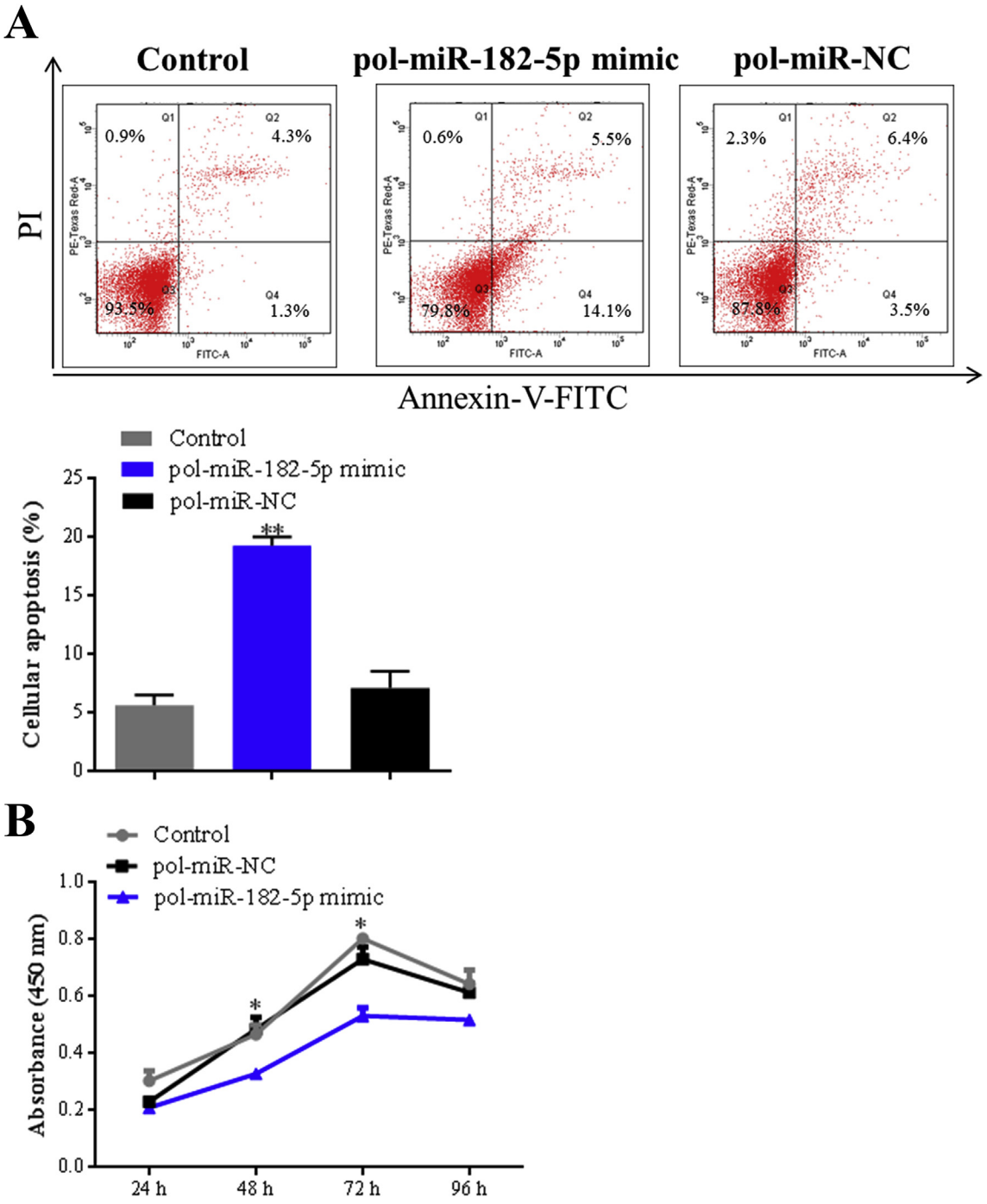

Fig. 4. Effect of pol-miR-182-5p on cellular apoptosis and viability. (A) FG-9307 cells were transfected with or without (control) pol-miR-182-5p mimic or pol-miR-NC for 48 h; the cells were labeled with annexin V-FITC and propidium iodide (PI), and apoptosis was determined by flow cytometry. The values in graphic representation are shown in the right panel. (B) FG-9307 cells were transfected as above, and the amount of viable cells was determined at different time points by measuring absorbance at 450 nm. Values are the means of triplicate experiments and shown as means ± SEM. **, $P < 0.01$; *, $P < 0.05$.

reduced compared to that in cells transfected with pMIR-182-5p-3′UTR$_{PoS1PR1}$ alone; in contrast, co-transfection with pMIR-182-5p-3′UTR$_{PoS1PR1}$ and the control miRNA, pol-miR-NC, had no significant effect on luciferase activity (Fig. 5A). To examine the specificity of the interaction between pol-miR-182-5p and 3′UTR$_{PoS1PR1}$, the reporter plasmid pMIR-182-5p-3′UTR$_{PoS1PR1}$-M was created, which bears a mutated 3′UTR$_{PoS1PR1}$ (Fig. S5). When HEK-293T cells were co-transfected with pMIR-182-5p-3′UTR$_{PoS1PR1}$-M and pol-miR-182-5p mimic, no reduction in luciferase activity was observed. Similar results were obtained with HEK-293T cells co-transfected with pMIR-182-5p-3′UTR$_{PoS1PR1}$ and pol-miR-182-5p mimic-M, the latter bearing a mutation in the seed sequence (Fig. 5B, Fig. S5). In the further investigation of the regulation effect of pol-miR-182-5p on PoS1PR1, it was found that in flounder FG-9307 cells transfected with pol-miR-182-5p mimic, but not with pol-miR-NC, PoS1PR1 expression was significantly reduced (Fig. 5C).

3.8. Sequence analysis of PoS1PR1

The function of PoS1PR1 has not been studied before. The protein

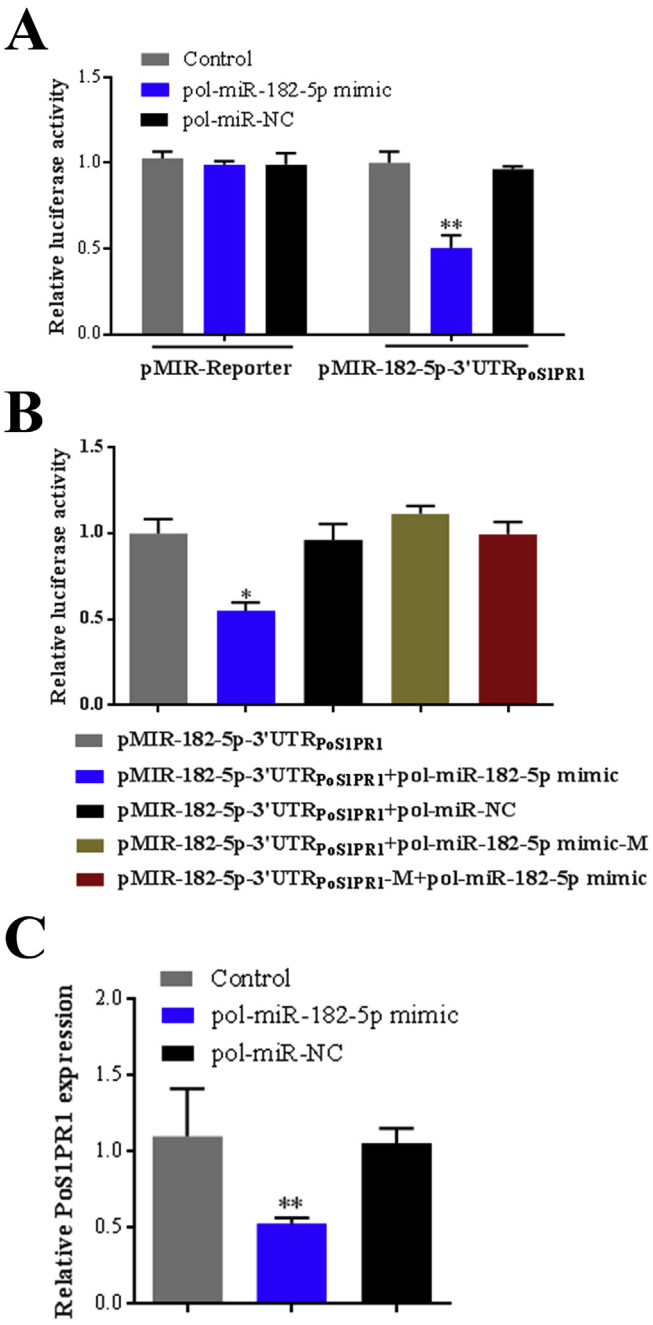

Fig. 5. Regulation of PoS1PR1 by pol-miR-182-5p. (A) HEK-293T cells were transfected with pMIR-182-5p-3′UTR$_{PoS1PR1}$ in the absence (control) or presence of pol-miR-182-5p mimic or pol-miR-NC. In parallel, HEK-293T cells were transfected with pMIR-Reporter in the absence (control) or presence of pol-miR-182-5p mimic or pol-miR-NC. Luciferase activity was determined at 24 h after transfection. Values are the means of triplicates and shown as means ± SD. **, $P < 0.01$. (B) HEK-293T cells were transfected with pMIR-182-5p-3′UTR$_{PoS1PR1}$ alone, pMIR-182-5p-3′UTR$_{PoS1PR1}$ plus pol-miR-182-5p mimic, pMIR-182-5p-3′UTR$_{PoS1PR1}$ plus pol-miR-NC, pMIR-182-5p-3′UTR$_{PoS1PR1}$ plus pol-miR-182-5p mimic-M, or pMIR-182-5p-3′UTR$_{PoS1PR1}$-M plus pol-miR-182-5p mimic. Luciferase activity was determined as above. (C) FG-9307 cells were transfected with or without (control) pol-miR-182-5p mimic or pol-miR-NC, and PoS1PR1 expression was determined by quantitative real time RT-PCR. Values are the means of triplicate experiments and shown as means ± SEM. **, $P < 0.01$; *, $P < 0.05$.

contains 409 amino acid residues with a calculated molecular mass of 45.64 kDa and a theoretical pI of 9.74. It was predicted to be a transmembrane G-protein-coupled receptor with seven transmembrane regions (residues from 65 to 87, 96 to 118, 133 to 155, 176 to 198, 218 to 240, 270 to 292, and 312 to 334). PoS1PR1 shares 63.4%-80.1% overall sequence identities with the S1PR1 of teleost including *Labeo rohita*, *Carassius auratus*, *Mastacembelus armatus*, *Cynoglossus semilaevis*, *Maylandia zebra*, *Oreochromis niloticus*, *Fundulus heteroclitus*, and *Oryzias melastigma* (Fig. 6). The overall sequence identities between PoS1PR1 and mouse and human S1PR1 are 49.1% and 48.2%, respectively (Fig. 6).

3.9. Effect of PoS1PR1 on E. tarda dissemination and invasion in flounder tissues

To examine the potential effect of PoS1PR1 on *E. tarda* infection, flounder with PoS1PR1 knockdown was created by injection into the fish the plasmid pPoS1PR1si and pPoS1PR1siC, which express PoS1PR1-specific and -nonspecific siRNA, respectively. qRT-PCR analysis indicated that at 5 d post-plasmid administration, PoS1PR1 mRNA levels in the head kidney, spleen, and liver of pPoS1PR1si-administered fish were significantly ($P < 0.01$) reduced to 60.7%, 53.3%, and 50.0%, respectively, of that in the control fish, whereas PoS1PR1 expression levels in pPoS1PR1siC-administered fish were similar to that in the control fish (Fig. S6). When flounder with pPoS1PR1si were infected with *E. tarda*, the bacterial numbers in kidney were significantly higher than that in the control fish at 12 and 48 hpi, the bacterial numbers in spleen were significantly higher than that in the control fish at 12 and 24 hpi, and the bacterial numbers in liver were significantly higher than that in the control fish at all time points (Fig. 7). In contrast, flounder containing pPoS1PR1siC showed no significant difference from the control fish in bacterial count.

4. Discussion

Many studies have demonstrated that host miRNA expression is markedly affected by bacterial infection [41,42]. In fish, such as tongue sole, large yellow croaker, and Japanese flounder, distinct miRNA expression profiles induced by bacterial, viral, and poly (I:C) treatment have been reported [34,35,43,44]. Recently, Liu et al. reported that *E. tarda* infection changed the expression of 17 miRNAs in liver [12]. Since head kidney is the most important immune organ of adult fish, we in this study examined the head kidney miRNA profiles during the course of *E. tarda* infection. We found that *E. tarda* caused 96 miRNAs (DEmiRNAs), most of which are novel miRNAs, to exhibit significantly altered expressions in a time dependent manner. The amount of the DEmiRNAs was highest at the relatively late stage (48 hpi) compared to the relatively early stage (12 and 24 hpi), and at each time point, more downregulated DEmiRNAs were detected than upregulated DEmiRNAs. It is possible that as the infection progressed, the battle between the invading bacteria and the defending host became intense and widerspread, which consequently involved more biological processes of the host, and thus more miRNAs were affected. The observation of higher amount of downregulated DEmiRNAs at each time point suggests that probably more activation than inhibition of target genes occurred during *E. tarda* infection, which may be a defense mechanism of the host to clear the pathogen.

Accumulating evidences have indicated that miRNAs exert their functions by negatively controlling the expression of their target genes [15,45]. In our study, a total of 2779 target genes were predicted for the 96 DEmiRNAs, indicating multiple targets for most of the miRNAs. Similarly, the number of predicted target genes for flounder liver miRNAs were much larger than the number of the miRNAs [12]. It is known that interactions between miRNAs and their target genes are vital for the maintenance of gene expression in an appropriate balance [8]. In our study, 87 of the DEmiRNAs-DEmRNAs pairs (involving 29 DE miRNAs and 86 DE mRNAs) correlated negatively in their expression profiles in a time-dependent fashion, suggesting that the DEmiRNAs-DEmRNAs interaction networks are temporally regulated by *E. tarda* in Japanese

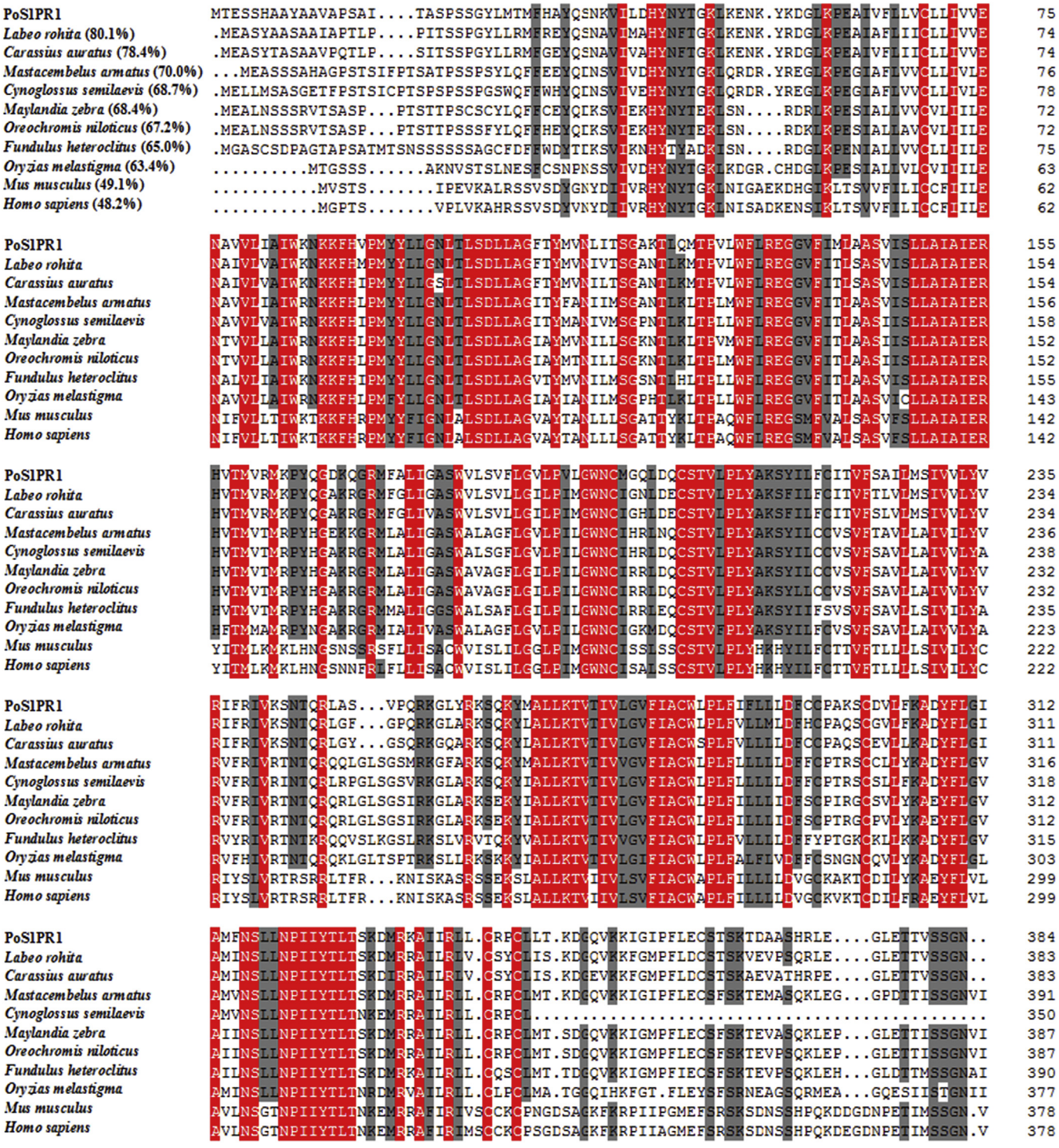

(caption on next page)

Fig. 6. Sequence alignment of PoS1PR1 homologues. Dots denote gaps introduced for maximum matching. Numbers in brackets indicate overall sequence identities between PoS1PR1 and the compared sequences. The consensus residues are in red, the residues that are ≥75% identical among the aligned sequences are in grey. The GenBank accession numbers of the aligned sequences are as follows: *Labeo rohita*, RXN19823.1; *Carassius auratus*, XP_026063351.1; *Mastacembelus armatus*, XP_026158572.1; *Cynoglossus semilaevis*, XP_008315817.1; *Maylandia zebra*, XP_014267173.1; *Oreochromis niloticus*, XP_003447975.1; *Fundulus heteroclitus*, XP_012705936.1; *Oryzias melastigma*, XP_024145398.1; *Mus musculus*, NP_031927.2; *Homo sapiens*, NP_001307659.1. (For interpretation of the references to colour in this figure legend, the reader is referred to the Web version of this article.)

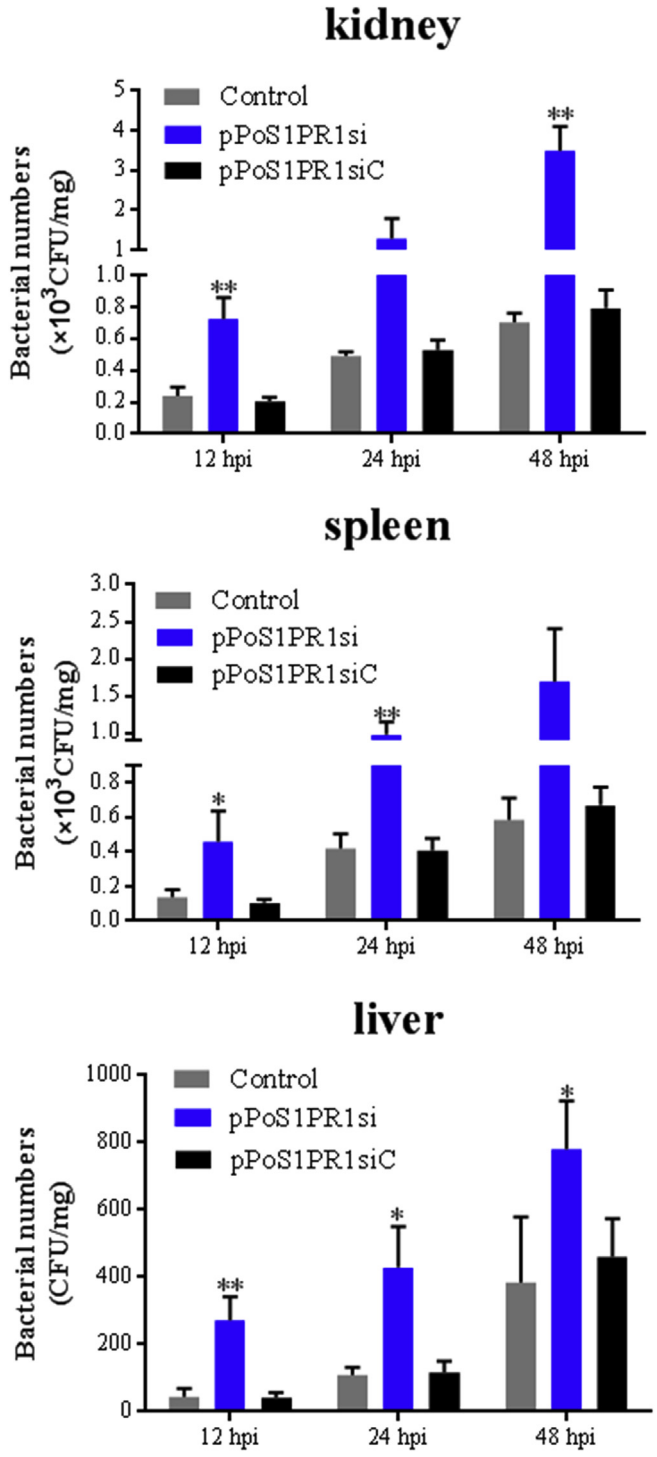

Fig. 7. Effect of PoS1PR1 on *Edwardsiella tarda* infection in flounder. Flounder with or without (control) PoS1PR1 knockdown were infected with *E. tarda*, and intracellular bacterial number in head kidney, spleen, and liver was determined at different time. Values are the means of triplicate experiments and shown as means ± SD. **, $P < 0.01$; *, $P < 0.05$.

flounder. Of the DEmRNAs predicted to be targeted by DEmiRNAs, GO and KEGG enrichment analysis showed that they were involved in diverse processes and pathways, including immune-related processes, notably B and T cell receptor signaling, p53 signaling pathway, lysosome, adhesion and attachment to host cell, and transmembrane receptor protein tyrosine kinase activity, all which likely contribute to the host's immune defense against pathogens. The expression patterns of these genes differed in different infection stages, suggesting a time-dependent regulation mechanism of flounder for the miRNAs repertoire during *E. tarda* infection.

Among the identified DEmiRNAs, pol-miR-182-5p showed continued and high level of upregulation from 12 hpi to 48 hpi both by high-throughput sequencing and stem-loop RT-PCR, suggesting a potentially important role of this miRNA in *E. tarda* infection. In mammals, miR-182-5p is known to act as a tumor-suppressor to suppress progression of renal cancer through cell cycle arrest by targeting lncRNA metastasis-associated lung adenocarcinoma transcript 1 (MALAT-1) [46]. However, another report showed that miR-182-5p enhances the motility and invasive ability of hepatocellular carcinoma cells by repressing FOXO3a, a member of Forkhead box O (FOXO) transcription factor family [47]. In lower vertebrates, studies on miR-182 are rare, except that one report showed that miR-182-5p was significantly downregulated in olive flounder under VHSV infection [48], which is consistent with our observation that miR-182-5p expression in Japanese flounder infected with megalocytivirus was downregulated significantly. In human prostate cancer cells, miR-182-5p is also known to inhibit the expression of anti-apoptotic proteins Bcl II and cell-cycle regulatory cyclin-dependent kinase inhibitors such as p21, thereby blocking cell regeneration [49]. Ectopic overexpression of miR-182-5p were found to induce apoptosis and cell-cycle arrest in epithelial cells [50,51]. Interestingly, another study showed that miR-182 could trigger TGF-β1-dependent NF-κB induction in glioma cells and provoke a more aggressive glioma phenotype by targeting the deubuiquitinase CYLB [52]. These observations suggest that miR-182 has a highly context-dependent activity, which largely depends on the cell type and genetic context [53]. In our study, we found that in FG cells transfected with pol-miR-182-5p mimic, apoptosis was enhanced and cell viability was reduced, suggesting that pol-miR-182-5p, when overexpressed, promoted fish cell apoptosis.

Luciferase reporter assay verified PoS1PR1 as the target gene of pol-miR-182-5p, as the latter interacted negatively with the 3′UTR of PoS1PR1 in a manner that depended on the specific seed sequence of pol-miR-182-5p. In mammals, sphingosine-1-phosphate receptor 1 (S1PR1) is one of the G protein-coupled receptors for sphingosine 1-phosphate (S1P) and plays an important role in a variety of developmental and biological processes including cell growth, survival, migration and immune responses [54,55]. S1P binds to its receptor (S1PR1 to S1PR5) and subsequently regulates various cellular effects [56]. Reports have indicated that S1PR1 signaling is indispensable in the suppression of excessive inflammation and protecting the host from immunopathology due to viral or bacterial infection [57–63]. S1PR1 could reduce the expression and secretion of pro-inflammatory cytokines in normal human epidermal keratinocyte when it was exposed to *S. aureus* invasion [64]. Similarly, for viral pathogens, S1PR1 agonists blunt the cytokine storm induced by influenza virus and respiratory syncytial virus [58,59], whereas S1PR1 antagonist decreased cytokine production in response to Newcastle disease virus infection [65]. However, S1PR1 function in fish is not known. In our study, in order to

investigate the function of flounder S1PR1 (PoS1PR1), RNAi-mediated PoS1PR1 knockdown was performed, which resulted in effective reduction in the expression of PoS1PR1 in three different tissues. Since the small RNA used in our study was expressed from a siRNA expression vector pRNAT-CMV3.1 (a eukaryotic plasmid that is designed to express siRNA in eukaryotic system including fish), it is likely that once being injected into fish, the plasmid was transported to various tissues where it entered into local cells and produced the encoded siRNA via the RNA synthesis machinery of the host cells, resulting in the inhibition of target gene expression in different tissues. This observation is similar to that of DNA vaccination, which has been widely accepted as an effective way of vaccination in mammals and fish. In DNA vaccination, a vaccine gene is encoded in a eukaryotic plasmid, which is introduced into fish usually via intramuscular injection, and the plasmid is then transported to various tissues, where the vaccine gene is expressed and the vaccine protein is synthesized, which subsequently induces systematic immune response. In the current study, we found that, when flounder with PoS1PR1 knockdown were infected with *E. tarda*, the bacterial number in fish tissues increased with time in a manner that was significantly faster than that in the control fish. These results indicated that PoS1PR1 is required for deterring bacterial invasion in fish. Given the function of S1PR1 in higher vertebrates and the effect of pol-miR-182-5p observed in our study, it is likely that downregulation of PoS1PR1 in flounder, effected by upregulated expression of pol-miR-182-5p, may lead to uncontrolled death of host cells, which enables the invading pathogen to disseminate rapidly in host tissues.

In summary, we in this study obtained the first global profile of *E. tarda*-induced host miRNAs expressed in Japanese flounder head kidney, which provides a valuable basis for future study of flounder miRNAs associated with *E. tarda* infection. Our results reveal an important role of pol-miR-182-5p as well as its target gene PoS1PR1 in the process of anti-*E. tarda* invasion, which adds new insights into the immune mechanism of teleost fish against bacterial infection.

Acknowledgements

This work was supported by the grants of the National Natural Science Foundation of China (31730100), the Shandong Major Science and Technology Innovation Project (2018SDKJ0302-2), the National Key R&D Program of China (2018YFD0900500), the AoShan Talents Program supported by Qingdao National Laboratory for Marine Science and Technology (No. 2015ASTP), and the Taishan Scholar Program of Shandong Province.

Appendix A. Supplementary data

Supplementary data to this article can be found online at https://doi.org/10.1016/j.fsi.2019.07.078.

References

[1] R.S. Pillai, S.N. Bhattacharyya, W. Filipowicz, Repression of protein synthesis by miRNAs: how many mechanisms? Trends Cell Biol. 17 (2007) 118–126.
[2] B. Wightman, I. Ha, G. Ruvkun, Posttranscriptional regulation of the heterochronic gene Lin-14 by Lin-4 mediates temporal pattern-formation in *C. elegans*, Cell 75 (1993) 855–862.
[3] D.P. Bartel, MicroRNAs: genomics, biogenesis, mechanism, and function, Cell 116 (2004) 281–297.
[4] D.P. Bartel, MicroRNAs: target recognition and regulatory functions, Cell 136 (2009) 215–233.
[5] M.R. Fabian, N. Sonenberg, W. Filipowicz, Regulation of mRNA translation and stability by microRNAs, Annu. Rev. Biochem. 79 (2010) 351–379.
[6] B.R. Cullen, MicroRNAs as mediators of viral evasion of the immune system, Nat. Immunol. 14 (2013) 205–210.
[7] G. Stefani, F.J. Slack, Small non-coding RNAs in animal development, Nat. Rev. Mol. Cell Biol. 9 (2008) 219–230.
[8] X. Zhang, X. Zhang, S.J. Hu, et al., Identification of miRNA-7 by genome-wide analysis as a critical sensitizer for TRAIL-induced apoptosis in glioblastoma cells, Nucleic Acids Res. 45 (2017) 5930–5944.
[9] Y. Zhang, W. You, H.M. Zhou, Downregulated miR-621 promotes cell proliferation via targeting CAPRIN1 in hepatocellular carcinoma, Am. J. Cancer Res. 8 (2018) 2116–2129.
[10] B.C. Zhang, Z.J. Zhou, L. Sun, pol-miR-731, a teleost miRNA upregulated by megalocytivirus, negatively regulates virus-induced type I interferon response, apoptosis, and cell cycle arrest, Sci. Rep. 6 (2016) 28354.
[11] X.L. Guan, B.C. Zhang, L. Sun, pol-miR-194a of Japanese flounder (*Paralichthys olivaceus*) suppresses type I interferon response and facilitates *Edwardsiella tarda* infection, Fish Shellfish Immunol. 87 (2019) 220–225.
[12] Y.Z. Liu, Y.X. Liu, M. Han, *Edwardsiella tarda*-induced miR-7a functions as a suppressor in PI3K/AKT/GSK3β signaling pathway by targeting insulin receptor substrate-2 (IRS2a and IRS2b) in Paralichthys olivaceus, Fish Shellfish Immunol. 89 (2019) 477–485.
[13] Z.X. Zhou, Z.J. Lin, X. Pang, et al., MicroRNA regulation of Toll-like receptor signaling pathways in teleost fish, Fish Shellfish Immunol. 75 (2018) 32–40.
[14] T.J. Xu, Q. Chu, J.X. Cui, et al., The inducible microRNA-203 in fish represses the inflammatory responses to Gram-negative bacteria by targeting IL-1 receptor-associated kinase 4, J. Biol. Chem. 293 (2018) 1386–1396.
[15] Q. Chu, Y.N. Sun, J.X. Cui, et al., MicroRNA-3570 modulates the NF-kB pathway in teleost fish by targeting MyD88, J. Immunol. 198 (2017) 3274–3282.
[16] W.J. Chen, L.Z. Yi, S.S. Feng, et al., Characterization of microRNAs in orange-spotted grouper (*Epinephelus coioides*) fin cells upon red-spotted grouper nervous necrosis virus infection, Fish Shellfish Immunol. 63 (2017) 228–236.
[17] C. Guo, H. Cui, S. Ni, et al., Comprehensive identification and profiling of host miRNAs in response to *Singapore grouper iridovirus* (SGIV) infection in grouper (*Epinephelus coioides*), Dev. Comp. Immunol. 52 (2015) 226–235.
[18] S.W. Ni, Y. Yan, H.C. Cui, et al., Fish miR-146a promotes *Singapore grouper iridovirus* infection by regulating cell apoptosis and NF-κB activation, J. Gen. Virol. 98 (2017) 1489–1499.
[19] K.Y. Leung, B.A. Siame, B.J. Tenkink, et al., *Edwardsiella tarda* virulence mechanisms of an emerging gastroenteritis pathogen, Microb. Infect. 14 (2012) 26–34.
[20] S.B. Park, T. Aoki, T.S. Jung, Pathogenesis of and strategies for preventing *Edwardsiella tarda* infection in fish, Vet. Res. 43 (2012) 67.
[21] P.S. Srinivasa Rao, T.M. Lim, K.Y. Leung, Opsonized virulent *Edwardsiella tarda* strains are able to adhere to and survive and replicate within fish phagocytes but fail to stimulate reactive oxygen intermediates, Infect. Immun. 69 (2001) 5689–5697.
[22] Y.H. Hu, Y.X. Li, L. Sun, *Edwardsiella tarda* Hfq: impact on host infection and global protein expression, Vet. Res. 45 (2014) 23.
[23] Y.H. Hu, L. Sun, The global regulatory effect of *Edwardsiella tarda* Fur on iron acquisition, stress resistance, and host infection: a proteomics-based interpretation, J. Proteom. 140 (2016) 100–110.
[24] F. Padrós, C. Zarza, L. Dopazo, et al., Pathology of *Edwardsiella tarda* infection in turbot, *Scophthalmus maximus* (L.), J. Fish Dis. 29 (2006) 87–94.
[25] X.P. Li, L. Sun, Toll-like receptor 2 of tongue sole *Cynoglossus semilaevis*: signaling pathway and involvement in bacterial infection, Fish Shellfish Immunol. 51 (2016) 321–328.
[26] N. Pirarat, T. Kobayashi, T. Katagiri, et al., Protective effects and mechanisms of a probiotic bacterium *Lactobacillus rhamnosus* against experimental *Edwardsiella tarda* infection in tilapia (*Oreochromis niloticus*), Vet. Immunol. Immunopathol. 113 (2006) 339–347.
[27] M. Yamasaki, K. Araki, T. Nakanishi, et al., Adaptive immune response to *Edwardsiella tarda* infection in ginbuna crucian carp, *Carassius auratus langsdorfii*, Vet. Immunol. Immunopathol. 153 (2013) 83–90.
[28] M.F. Li, L. Sun, J. Li, *Edwardsiella tarda* evades serum killing by preventing complement activation via the alternative pathway, Fish Shellfish Immunol. 43 (2015) 325–329.
[29] Z.J. Zhou, L. Sun, *Edwardsiella tarda*-induced inhibition of apoptosis: a strategy for intracellular survival, Front. Cell. Infect. Microbiol. 6 (2016) 76.
[30] J.J. Wang, L. Sun, Edwardsiella tarda-regulated proteins in Japanese flounder (*Paralichthys olivaceus*): identification and evaluation of antibacterial potentials, J. Proteom. 124 (2015) 1–10.
[31] Z.J. Zhou, L. Sun, CsCTL1, a teleost C-type lectin that promotes antibacterial and antiviral immune defense in a manner that depends on the conserved EPN motif, Dev. Comp. Immunol. 50 (2015) 69–77.
[32] H.R. Wang, Y.H. Hu, W.W. Zhang, et al., Construction of an attenuated Pseudomonas fluorescens strain and evaluation of its potential as a cross-protective vaccine, Vaccine 27 (2009) 4047–4055.
[33] K. Sun, H.L. Wang, M. Zhang, et al., Genetic mechanisms of multi-antimicrobial resistance in a pathogenic *Edwardsiella tarda* strain, Aquaculture 289 (2009) 134–139.
[34] R. Qiu, J. Li, Z.Z. Xiao, et al., Macrophage migration inhibitory factor of *Sciaenops ocellatus* regulates immune cell trafficking and is involved in pathogen induced immune response, Dev. Comp. Immunol. 40 (2013) 232–239.
[35] B.C. Zhang, J. Zhang, L. Sun, In-depth profiling and analysis of host and viral microRNAs in Japanese flounder (*Paralichthys olivaceus*) infected with megalocytivirus reveal involvement of microRNAs in host-virus interaction in teleost fish, BMC Genomics 15 (2014) 878.
[36] Y.S. Fu, Z.Y. Shi, M.L. Wu, et al., Identification and differential expression of microRNAs during metamorphosis of the Japanese flounder (*Paralichthys olivaceus*), PLoS One 6 (2011).
[37] S.L. Tong, H. Li, H.Z. Miao, The establishment and partial characterization of a continuous fish cell line FG-9307 from the gill of flounder *Paralichthys olivaceus*, Aquaculture 156 (1997) 327–333.
[38] Z.X. Zhou, B.C. Zhang, L. Sun, Poly (I: C) induces antiviral immune responses in Japanese flounder (Paralichthys olivaceus) that require TLR3 and MDA5 and is negatively regulated by Myd88, PLoS One 9 (2014).

[39] X.P. Li, L. Sun, TLR7 is required for optimal immune defense against bacterial infection in tongue sole (*Cynoglossus semilaevis*), Fish Shellfish Immunol. 47 (2015) 93–99.
[40] W.J. Zheng, L. Sun, Evaluation of housekeeping genes as references for quantitative real time RT-PCR analysis of gene expression in Japanese flounder (*Paralichthys olivaceus*), Fish Shellfish Immunol. 30 (2011) 638–645.
[41] H.Y. Hu, B.C. Zhang, H.Z. Zhou, et al., *Edwardsiella tarda*-induced miRNAs in a teleost host: global profile and role in bacterial infection as revealed by integrative miRNA–mRNA analysis, Virulence 8 (2017) 1457–1464.
[42] J.J. Han, G.L. Xu, T.J. Xu, The miiuy croaker microRNA transcriptome and microRNA regulation of RIG-I like receptor signaling pathway after poly (I: C) stimulation, Fish Shellfish Immunol. 54 (2016) 419–426.
[43] Z.X. Sha, G.Y. Gong, S.L. Wang, et al., Identification and characterization of *Cynoglossus semilaevis* microRNA response to *Vibrio anguillarum* infection through high-throughput sequencing, Dev. Comp. Immunol. 44 (2014) 59–69.
[44] P.Z. Qi, B.Y. Guo, A.Y. Zhu, et al., Identification and comparative analysis of the *Pseudosciaena crocea* microRNA transcriptome response to poly (I: C) infection using a deep sequencing approach, Fish Shellfish Immunol. 39 (2014) 483–491.
[45] Y.Q. Zhou, Z.C. Xia, Z.K. Cheng, et al., Inducible microRNA-590-5p inhibits host antiviral response by targeting the soluble IL-6 receptor, J. Biol. Chem. 293 (2018) 18168–18179.
[46] P. Kulkarni, P. Dasgupta, S. Majid, et al., miR-182-5p suppresses progression of renal cancer through cell cycle arrest by targeting lncRNA MALAT-1, Cancer Res. 78 (2018) 14–18.
[47] M.Q. Cao, A.B. You, X.D. Zhu, et al., miR-182-5p promotes hepatocellular carcinoma progression by repressing FOXO3a, J. Hematol. Oncol. 11 (2018).
[48] A. Najib, M.S. Kim, S.H. Choi, et al., Changes in microRNAs expression profile of olive flounder (*Paralichthys olivaceus*) in response to viral hemorrhagic septicemia virus (VHSV) infection, Fish Shellfish Immunol. 51 (2016) 384–391.
[49] X.J. Peng, W.P. Li, L. Yuan, et al., Inhibition of proliferation and induction of autophagy by atorvastatin in PC3 prostate cancer cells correlate with downregulation of Bcl2 and upregulation of miR-182 and p21, PLoS One 8 (2013).
[50] A. Rihani, A.V. Goethem, M. Ongenaert, et al., Genome wide expression profiling of p53 regulated miRNAs in neuroblastoma, Sci. Rep. 5 (2015) 9027.
[51] K. Krishnan, A.L. Steptoe, H.C. Martin, et al., MicroRNA-182-5p targets a network of genes involved in DNA repair, RNA 19 (2013) 230–242.
[52] L.B. Song, L.P. Liu, Z.Q. Wu, et al., TGF-β induces miR-182 to sustain NF-κB activation in glioma subsets, J. Clin. Investig. 122 (2012) 3563–3578.
[53] F.M. Kouri, L.A. Hurley, W.L. Daniel, et al., miR-182 integrates apoptosis, growth, and differentiation programs in glioblastoma, Genes Dev. 29 (2015) 732–745.
[54] N.J. Pyne, S. Pyne, Sphingosine 1-phosphate and cancer, Nat. Rev. Cancer 10 (2010) 489–503.
[55] V.A. Blaho, T. Hla, Regulation of mammalian physiology, development, and disease by the sphingosine 1-phosphate and lysophosphatidic acid receptors, Chem. Rev. 111 (2011) 6299–6320.
[56] C. Skerry, K. Scanlon, J. Ardanuy, et al., Reduction of pertussis inflammatory pathology by therapeutic treatment with sphingosine-1-phosphate receptor ligands by a pertussis toxin-insensitive mechanism, J. Infect. Dis. 215 (2017) 278–286.
[57] M. Aoki, H. Aoki, R. Ramanathan, et al., Sphingosine-1-phosphate signaling in immune cells and inflammation: roles and therapeutic potential, Mediat. Inflamm. (2016), https://doi.org/10.1155/2016/8606878.
[58] J.R. Teijaro, K.B. Walsh, S. Cahalan, et al., Endothelial cells are central orchestrators of cytokine amplification during influenza virus infection, Cell 146 (2011) 980–991.
[59] K.B. Walsh, J.R. Teijaro, L.G. Brock, et al., Animal model of respiratory syncytial virus: CD8+ T cells cause a cytokine storm that is chemically tractable by sphingosine-1-phosphate 1 receptor agonist therapy, J. Virol. 88 (2014) 6281–6293.
[60] X.Q. Xu, C.M. Huang, Y.F. Zhang, et al., S1PR1 mediates anti-apoptotic/pro-proliferative processes in human acute myeloid leukemia cells, Mol. Med. Rep. 14 (2016) 3369–3375.
[61] J.N. Zhao, M.Y. Zhu, H. Jiang, et al., Combination of sphingosine-1-phosphate receptor 1 (S1PR1) agonist and antiviral drug: a potential therapy against pathogenic influenza virus, Sci. Rep. 9 (2019) 5272.
[62] S. Sammani, L.M. Vinasco, T. Mirzapoiazova, et al., Differential effects of sphingosine 1-phosphate receptors on airway and vascular barrier function in the murine lung, Am. J. Respir. Cell Mol. Biol. 43 (2010) 394–402.
[63] V.K. Konvalinkova, S. Yasuda, T. Rubic, et al., Stable knock-down of the sphingosine 1-phosphate receptor S1P1 influences multiple functions of human endothelial cells, Arterioscler. Thromb. Vasc. Biol. 25 (2005) 546–552.
[64] S. Igawa, J.E. Choi, Z.P. Wang, et al., Human keratinocytes use sphingosine 1-phosphate and its receptors to communicate *S. aureus* invasion and activate host defense, J. Investig. Dermatol. 139 (2019) 1743–1752.
[65] Y.L. Li, P. Xie, M.H. Sun, et al., S1PR1 expression correlates with inflammatory responses to Newcastle disease virus infection, Infect. Genet. Evol. 37 (2016) 37–42.